Appl. Phys. B 76, 457–465 (2003)
DOI: 10.1007/s00340-003-1126-6

Applied Physics B
Lasers and Optics

Fluorescence lidar imaging of the cathedral and baptistery of Parma

D. LOGNOLI[1]
G. CECCHI[1,✉]
I. MOCHI[1]
L. PANTANI[1]
V. RAIMONDI[1]
R. CHIARI[2]
T. JOHANSSON[3]
P. WEIBRING[3]
H. EDNER[3]
S. SVANBERG[3]

[1] CNR–Institute of Applied Physics “Nello Carrara”, Via Panciatichi 64, 50127 Firenze, Italy
[2] Institute of Petrography, Department of Earth Sciences, University of Parma, Viale delle Scienze 78, 43100 Parma, Italy
[3] Department of Physics, Lund Institute of Technology, P.O. Box 118, 221 00 Lund, Sweden

Received: 24 July 2002/Revised version: 16 January 2003

ABSTRACT Extensive fluorescence multispectral imaging of the cathedral and baptistery of Parma, Italy, is reported and discussed. In particular, the first fluorescence imaging data from protection-treated stony materials were recorded. Fluorescence spectra were taken with a mobile lidar system scanning the monument surfaces with a frequency-tripled Nd:YAG laser beam from a distance of about 80 m. For each pixel of the area investigated, a high-spectral-resolution spectrum in the full visible range was acquired. The principal-component analysis technique was used to obtain thematic maps that outlined areas subject to protective treatment and biological growth, and other features, such as different types of stones and decoration pigments.

PACS 42.62.Fi; 42.79.Qx

1 Introduction

Cultural heritage conservation is an important issue that has a great impact on several aspects of our life, from cultural aspects to economical ones. Historical buildings are a considerable part of our cultural heritage. However, the damage assessment and, in general, the control of the conservation status of a monument is a complex issue that involves the investigation and measurement of many parameters. In many cases these tasks also require the acquisition of samples and the subsequent analysis in the laboratory. Hence, extensive control of historical building heritage can require considerable resources in terms of time, money and specialised personnel. Moreover, the acquisition of samples implies a violation of the integrity of the monument and a manipulation of the original material. In some cases this may lead to artefacts in the results, for example stone samples with spores or quiescent forms that become active only once isolated and cultivated in the laboratory; hence the increasing importance given to the development of in situ and non-destructive techniques for the monitoring of cultural heritage.

The laser-induced fluorescence (LIF) technique is widely applied in many fields of scientific investigation and even in every-day life, since it can allow the detection of features that are not visible with the naked eye or be used for the characterisation of different substances by means of their fluorescence spectral signatures [1, 2]. It is also used in the field of cultural heritage, especially for painting inspection [3] and fluorescence microscopy [4]. Fluorescence lidar remote sensing [5] allows the application of the LIF technique in the outdoor environment. With respect to the traditional in situ techniques it offers the further advantage of operation from a remote location, thus allowing the control of areas that are difficult to reach without scaffolding.

Fluorescence lidar remote sensing has recently been demonstrated as a helpful tool for a quick measurement of several indicators that may be used to assess the conservation status of a historical building [6–8]. First field experiments were conducted on the Parma baptistery in 1994, where a fluorescence lidar system was used for point monitoring of different lithotypes on the facade [9]. In the following years further experiments investigated fluorescence lidar remote sensing potentials for the characterisation of biodeteriogens on stone materials [7, 10], for the characterisation of protective treatments on samples prepared in the laboratory [11] and the effects of biocide treatments [12]. It was not until 1997, however, that the first experiment of lidar multispectral imaging was performed [13]. The study concerned Lund Cathedral, Sweden, for which a single area (8 m × 8 m) on the northern facade of the cathedral was investigated by using the lidar multispectral imaging technique. The experiment mainly concerned the investigation of the fluorescence signatures of Höör quartzitic sandstone, which was used for the ashlars of the cathedral’s main stone masonry, and the detection of biodeteriogens. The results showed good potential for achieving thematic maps aimed at the characterisation of the lithotypes and the detection and characterisation of biodeteriogens.

Fluorescence thematic maps are particularly attractive for the control of monuments, firstly because they furnish a piece of information that has a comprehensive relevance to the status of the whole monument and a spatial definition that cannot be obtained by means of mere sampling. Moreover, the opportunity of recording time-dependent, repetitive fluorescence images opens new prospects for reliable control of the status changes of the monument. Another important aspect of thematic maps is that they make it easier to transfer the knowledge gained, with a sophisticated analysis of the fluo-

---

✉ Fax: +39-055/410-893, E-mail: g.cecchi@ifac.cnr.it

TABLE 1 Dimensions of the areas monitored and other related scanning data

Baptistery

Area Label	Number of pixels horizontal	vertical	Total	Laser Spot Diameter	Pixel step horizontal	vertical	Total surface area
Area A	67	72	4824	6 cm	12 cm	12 cm	69.5 m^2
Area B	60	60	3600	6 cm	12 cm	12 cm	51.8 m^2
Area C	75	75	5625	6 cm	6 cm	6 cm	20.2 m^2
Area L	50	71	3550	6 cm	12 cm	12 cm	51.1 m^2

Cathedral

Area Label	Number of pixels horizontal	vertical	Total	Laser Spot Diameter	Pixel step horizontal	vertical	Total surface area
Area D	75	74	5550	6 cm	12 cm	12 cm	79.9 m^2
Area E	68	68	4624	6 cm	12 cm	12 cm	66.6 m^2
Area F	70	70	4900	6 cm	12 cm	12 cm	70.6 m^2
Area G	70	70	4900	6 cm	9 cm	9 cm	39.7 m^2
Area H	70	70	4900	6 cm	12 cm	12 cm	70.6 m^2
Area I	60	60	3600	6 cm	12 cm	12 cm	51.8 m^2
Area J	70	70	4900	6 cm	6 cm	6 cm	70.6 m^2
Area K	70	10	700	6 cm	12 cm	12 cm	10.1 m^2

rescence data, which necessarily requires a specific scientific background, to the conservation specialist and/or to the decision maker.

The present work aims at extending the results obtained in the only fluorescence lidar imaging experiment on monuments previously conducted [13] by addressing the following specific goals:

a) investigation of the practicability of the detection of protective treatments in the field;
b) enhancement of the feasibility of identifying different lithotypes including different types of limestones, marbles and sandstones;
c) exploitation of the potential of the lidar multispectral imaging technique for extensive monitoring of historical buildings.

2 Experimental

The experiment was performed in Parma in September 2000. The cathedral and the baptistery of Parma are two of the most interesting medieval buildings in northern Italy.

The cathedral (Fig. 1a) is a composite building in the Romanesque style. It was built before AD 1046 and, after the earthquake of AD 1117, it was partially rebuilt. The reconstruction ended around AD 1294 with the erection of the bell tower. The facade is made of ashlars of different whitish and yellowish stones, mainly different types of arenites (e.g. ostia, sporno, pietraforte) and limestones and marbles (e.g. rosso veronese, bardiglio, rosa corallo). The facade's lower part shows three doorways. The central doorway is surmounted by a marble porch (protiro) decorated with carved figures. The upper part of the facade is decorated with three orders of small arches. Some parts of the facade, particularly on the right side, are colonised by biodeteriogens or show black crusts. The marble porch was treated with a protective treatment in the 1990s.

The baptistery (Fig. 1b) is considered to be one of the most beautiful buildings of the transition period between the Romanesque and Gothic styles. Its construction started in AD 1196 and ended in AD 1259. Archive data regarding the building of the baptistery tell of a break in the construction work of approximately twenty years, and completion of the building, particularly with regards to its embellishment with coating slabs, pillars, and bas-reliefs, around AD 1259. The decoration of the upper part was completed in 1307. It has an octagonal structure with four orders of open arches and a fifth order of blind arches. It is completely covered with slabs of rosso veronese, a limestone widely employed as decorative material due to its colour and typical texture. The lower part of the building has three carved doorways. The baptistery underwent a recent restoration intervention including stone cleaning and a protective treatment different from that used for the protiro.

Both these monuments were chosen as targets for the first lidar experiment held in 1994 [9]. The earlier measurements were restricted to a limited set of point measurements and are now complemented with extensive fluorescence imaging with an emphasis on the monitoring of protective treatments.

The measurements were performed using the Lund Laser Centre's mobile lidar system. This lidar system, which is adapted primarily for atmospheric monitoring [14], has recently undergone a substantial upgrading [15]. The measurement routines were similar to those described in a previous paper [13]. The general optical and electronic layout of the system is shown in Fig. 2. Frequency-tripled Nd:YAG laser pulses at 355 nm were transmitted at 20 Hz and at a typical pulse energy of 30 mJ towards the monuments via a scanning roof-top mirror. Fluorescence light was collected with a 40-cm diameter, 1-m focal length Newtonian telescope and focused into an optical fibre bundle, conveying the light with circular to linear geometrical transformation to the entrance slit of a spectrometer equipped with a gated and intensified CCD detector. The recorded spectrum was stored for each illuminated target spot for subsequent analysis.

During the experiment, 12 areas of the two monuments were monitored: 8 areas on the cathedral and 4 areas on the baptistery. The locations of the monitored areas are shown in Fig. 1a and b. The concept of the multispectral imaging measurement is shown in Fig. 3: each area was scanned with the

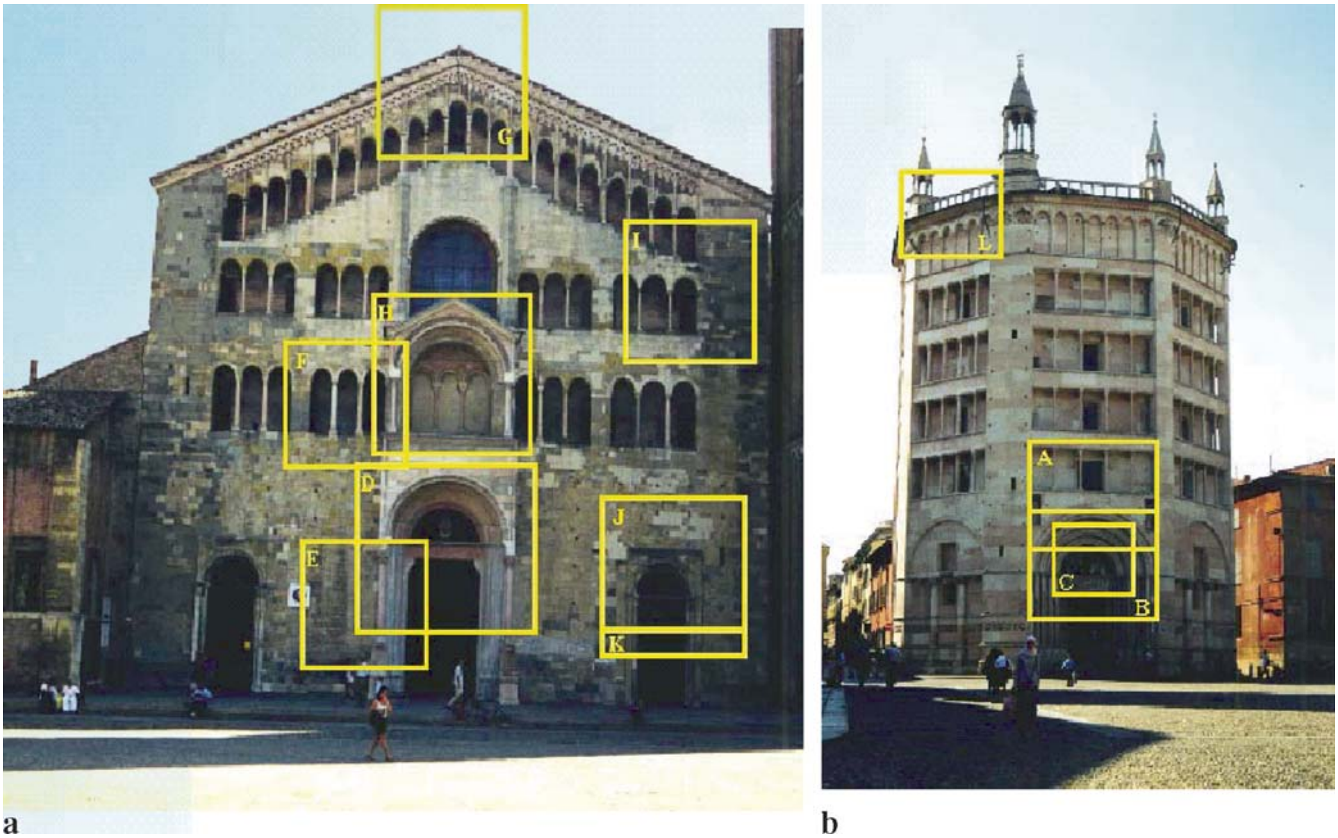

FIGURE 1 Scenario for the fluorescence lidar multispectral imaging experiment in Parma: the cathedral (**a**) and the baptistery (**b**). The *squares* indicate the areas investigated, which are labelled A, B, C, etc

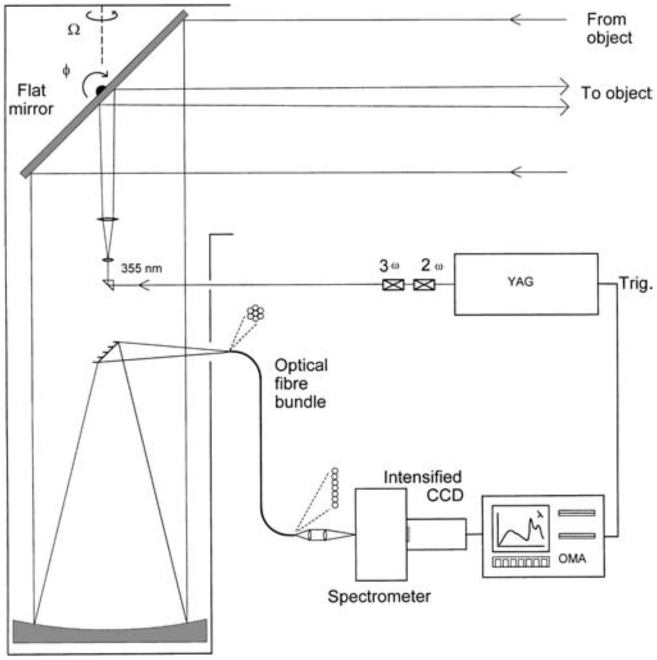

FIGURE 2 Optical and electronic arrangements of the mobile lidar system employed for the fluorescence multispectral imaging measurements: OMA, optical multichannel analyser

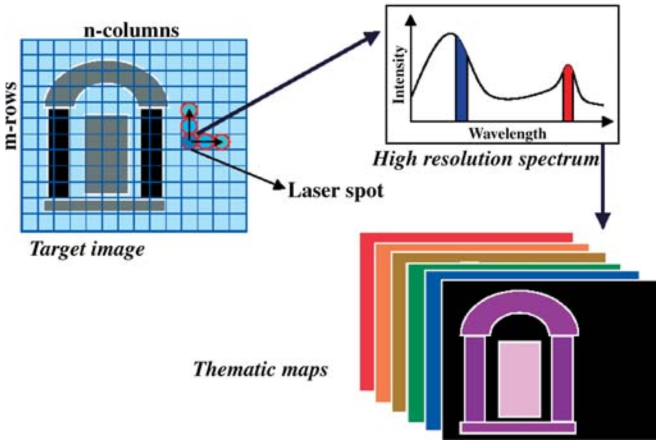

FIGURE 3 Basic principles of lidar multispectral imaging on monuments: the area investigated on the surface of the monument can be ideally divided into $m \times n$ 'squares' and then scanned with the lidar system to obtain an image of the target. For each 'square' of the target image a full high-resolution fluorescence spectrum is acquired. The laser beam expander can be adjusted so as to cover the whole 'square' or just a part of it. The $m \times n$ set of fluorescence spectra is finally analysed to obtain thematic maps that outline specific fluorescence features of the target

lidar system in order to obtain a matrix constituted of $m \times n$ pixels, each pixel being constituted by a high-resolution fluorescence spectrum ranging from 395 to 715 nm with a spectral resolution of approximately 10 nm. The lidar system was equipped with stepper motors driving the mirror scanning the target. The number of horizontal and vertical steps of the motors was chosen so that the spatial resolution on the target areas A through L were as specified in Table 1. In the following, 'X-m.n' indicates the fluorescence spectrum corresponding to the *m*th row and *n*th column of the area X.

Each spectrum was acquired after accumulating fluorescence data over 3–12 laser shots. The ambient background was acquired at the beginning of each set of measurements and then subtracted. The lidar system was placed at about 80 m from the two targets. Such a distance ensured a small scanning angle on the target so that the differences in the size of the laser footprint were negligible.

3 Multispectral imaging measurements

Figure 4 presents five fluorescence spectra showing some typical features found in the multispectral measurements. The spectra were collected in different areas of the baptistery and cathedral. The spectra were normalised at their corresponding maximum in the range 395 to 650 nm to outline the different spectral shapes.

The curve (a) presents the spectrum collected in pixel D-74.3 and shows very strong fluorescence in the shorter wavelength region of the spectrum. This spectral feature at 400 nm is due to the presence of protective treatment on the stone, which in this case is a marble (bardiglio).

The curve (b) refers to the spectrum of the pixel L-20.5: in the red region the spectrum shows the typical fluorescence peak of chlorophyll at 680 nm, thus indicating a strong presence of biodeteriogens. The stone substrate is a calcareous stone, rosso veronese.

The curve (c) presents the spectrum of the pixel B-16.12. The stone is a whitish slab of rosso veronese. These spectral features are very similar to those detected during the previous experiment carried out in 1994 [9].

The curve (d) presents the spectrum for the pixel B-32.2. This spectrum refers to a reddish slab of rosso veronese. The spectral shape is slightly different from that in curve (c) due to a higher contribution to fluorescence in the 500–600-nm region, which is typical of reddish slabs of rosso veronese.

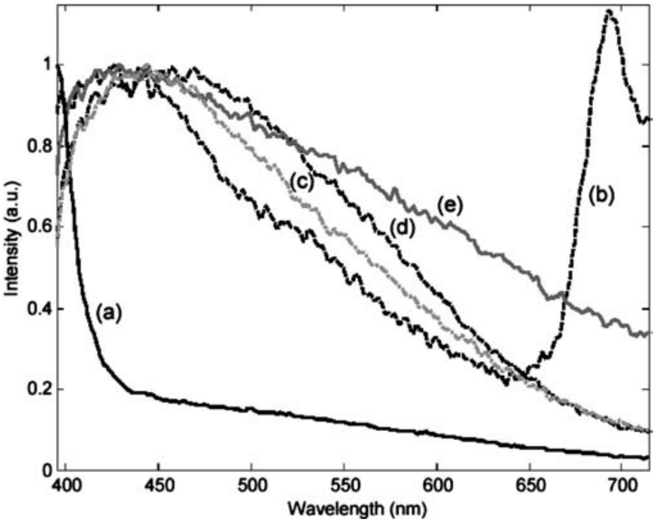

FIGURE 4 Five typical fluorescence spectra collected from different points on the two monuments: (a) bardiglio marble subject to protective treatment (pixel D-74.3); (b) rosso veronese limestone with biodeteriogens (pixel L-20.5); (c) rosso veronese limestone (pixel B-16.12); (d) rosso veronese limestone (pixel B-32.2); and (e) bardiglio marble (pixel D-54.61)

The curve (e) presents the spectrum of the pixel D-54.61. This refers to a marble (bardiglio) and shows a maximum at shorter wavelengths (approximately 420 nm) with respect to the other types of stones and still strong fluorescence contributions in the red region.

4 Data analysis and discussion of the results

The high-resolution fluorescence spectra collected for each pixel of the scanned areas listed in Table 1 can be used to obtain thematic maps, pointing out the main characteristics shown in the spectrum.

4.1 *Method description*

A rather straightforward method to produce a thematic map from a set of spectra is the so-called ratio imaging. The value of the ratio between the intensities of specific fluorescence bands is associated with each point of the image. The bands are chosen in order to obtain information on a certain characteristics of the target. This method is very simple and quick; besides, it provides a way to remove many problems related to the observation geometry. The main disadvantage of this technique is the difficulty of approaching the analysis of spectra with unknown characteristics; that is, the technique requires a basic knowledge of the spectral features of the parameters investigated in order to choose the bands correctly and/or to separate different fluorescence contributions in the same spectral region.

A different approach for information retrieval from the fluorescence spectra is to use PCA analysis [16, 17]. PCA analysis is a projection of the spectral information onto a lower dimensional subspace. This subspace is built-up by a set of orthogonal principal components (PCs), where the PCs are chosen in such a way that the first PC describes as much of the covariance among the samples as possible, the second PC as much of the residual covariance and so on. New PCs are added until the residual is considered as just noise. Each PC can be described by a loading vector. The loading vector is a projection vector, or a link between the original variables and the PC. An individual sample is then described by its new coordinates in the space spanned by the PCs with the expansion coefficients forming a score vector.

The thematic map related to a specific parameter can be obtained by converting the scores of the relevant PC in a grey scale or in a false-colour set.

4.2 *Thematic maps*

Figure 5 shows a picture of area H on the cathedral (Fig. 5a) and three thematic maps (Fig. 5b, c and d). The first thematic map (Fig. 5b) is obtained by calculating the ratio between the integrated area in the range 396 to 409 nm and that in the range 410 to 448 nm. In this way the map points out in yellow/red colours the areas where there is still some protective treatment. The fluorescence spectrum of these pixels is very similar to the spectrum of the pixel D-74.3 shown in Fig. 4 (curve (a)). Figure 5c and d presents thematic maps obtained with the PCA method. Figure 5e shows the shapes of the PC1, PC2 and PC3. The PCA analysis was applied in the range between 412 nm and 708 nm. This range was selected so

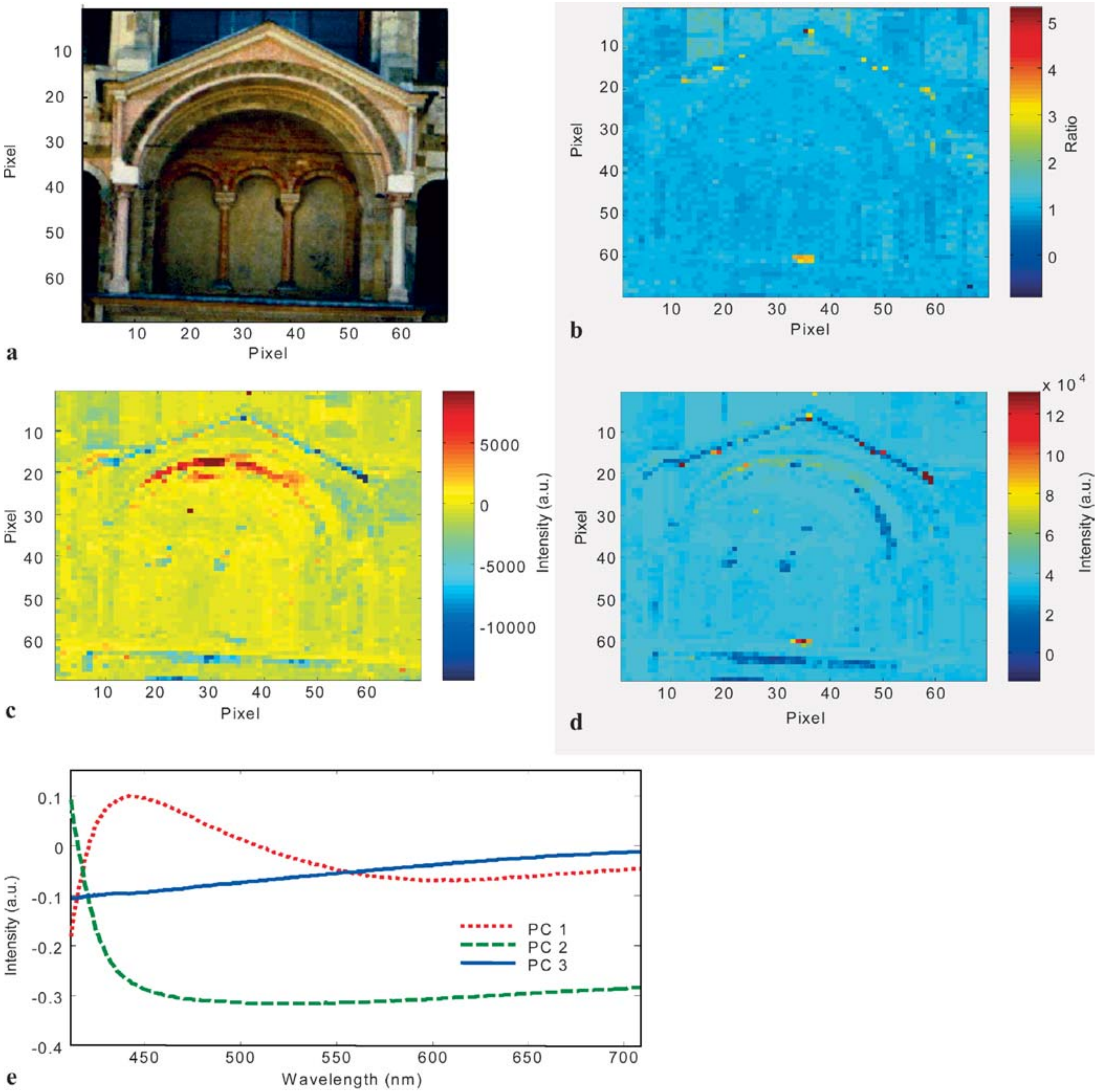

FIGURE 5 Area H of the cathedral: fluorescence data were analysed by calculating the ratio between integrated areas of the spectrum and by the PCA method, to put in evidence the areas subject to protective treatment. **a** A picture of the area investigated. **b** A thematic map obtained from the ratio of the integrated area in the range 396 to 409 nm and the integrated area in the range 410 to 448 nm. **c** The thematic map obtained from the scores associated with the PC3. **d** The thematic map obtained from the scores associated with the PC2. **e** Shapes of the PC1, PC2 and PC3

as to exclude the spectral region where the fluorescence of the treatment was strongly dominant over the typical stone signal. The PC1, PC2 and PC3 explain 94.4%, 4.5% and 0.9% of the total variance, respectively. Two of the first three PCs, however, are dominated by the fluorescence of the treatment, which generates most of the total variance. PC1 is affected by the fluorescence of the treatment in the first part of the shape and by the fluorescence of the stones at longer wavelengths. PC2 can be easily associated with the treatment, but still has a small contribution from the stones. PC3 is not affected by the treatment and can be used to describe the properties of the stones. Figure 5c shows the scores associated with the PC3. Figure 5d shows the scores associated with the PC2 and then enhances the areas where there are traces of protective treatment. This can be compared with the map in Fig. 5b. The map of Fig. 5d shows the limitation of the representation obtained with the PCA method: PC2, and consequently the relative map, contains residual information on stones. The reason for this is that the set of PCs does not have a correspondence with the physical properties of the targets.

Figure 6 shows fluorescence spectra referring to the yellow pixels pointed out in the thematic map of Fig. 5b (the

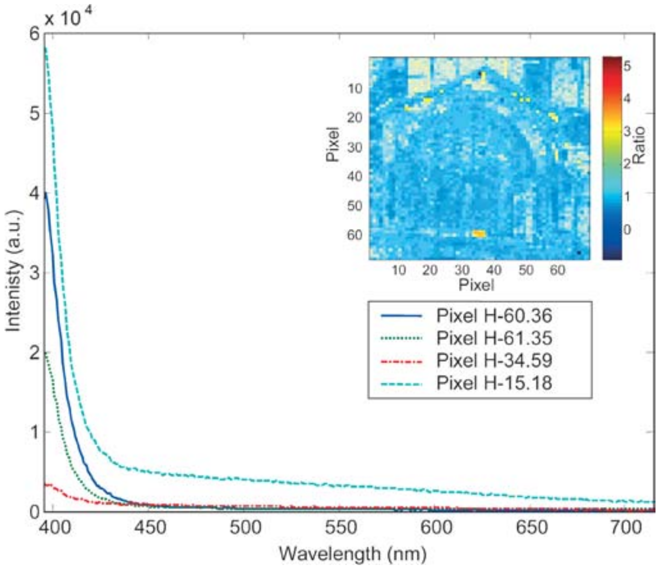

FIGURE 6 Fluorescence spectra corresponding to yellow pixels in the thematic map of Fig. 5b: the spectra show fluorescence due to the protective treatment. The thematic map is also given in the *inset*

latter is also shown in the inset of Fig. 6). The spectra show a very strong fluorescence in the shorter-wavelength region of the spectrum due to the protective treatment. The fluorescence signal due to the protective treatment is very intense in comparison with the fluorescence due to the stone (bardiglio marble). The fluorescence features of the stone appear as a broad weak distribution at longer wavelengths.

The presence of residual protective treatment is more marked in the area around the protiro of the Cathedral, especially in those areas that are less subject to weathering. Figure 7a and b shows, respectively, a picture of the protiro of the cathedral (area D in Fig. 1a and Table 1) and a thematic map built so as to enhance the protective treatment. This map is obtained by calculating the ratio between the integrated area in the range 396 to 408 nm and that in the range 409 to 450 nm. The blue pixels refer to areas free from treatment, while the yellow-red ones refer to areas still covered with treatment. The latter are usually the more internal areas protected by the protiro against rainfall. The fluorescence spectra corresponding to yellow-red pixels in this area (bottom left of Fig. 7b) are shown in Fig. 7c: the spectra show a strong signal due to the protective treatment. Fluorescence spectra that still indicate the presence of protective treatment but in a lower degree are shown in Fig. 7d: the residual protective treatment brings about the fluorescence peak just below 400 nm while the fluorescence features of the stone (bardiglio marble) are represented by the broad fluorescence band at longer wavelengths. The spectra were taken in the area at the bottom right in Fig. 7a.

The same area around the protiro was also investigated with a different mobile lidar system, the FLIDAR-3 developed at the CNR-IFAc, which features an excimer laser at 308 nm as an excitation source. The system can perform only point fluorescence measurements since presently it is not equipped with a scanning system. A complete description of the system can be found in [18, 19]. Figure 8a displays the spots where the point fluorescence measurements were taken. The results obtained exciting at 308 nm are shown in Fig. 8a: the fluores-

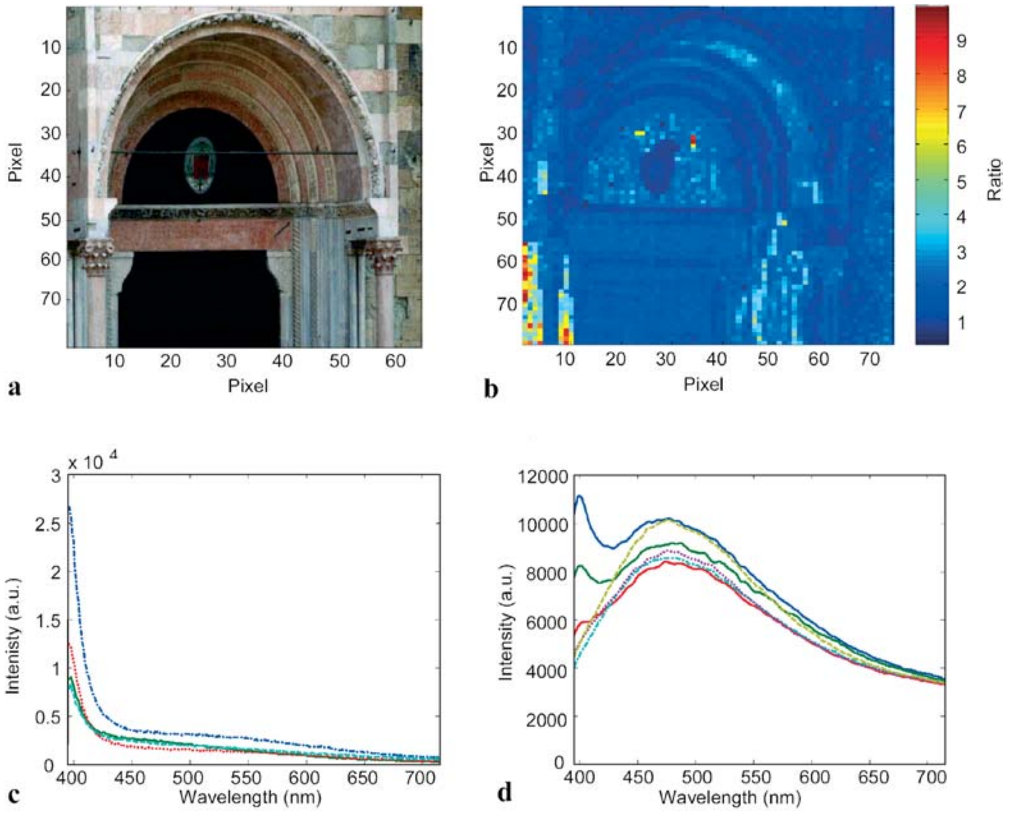

FIGURE 7 Area D of the cathedral: **a** a picture of the area investigated; **b** the thematic map obtained from the ratio between the integrated area in the range 396 to 408 nm and the integrated area in the range 409 to 450 nm; the *yellow-red areas* in the image indicate areas subject to protective treatment; **c** fluorescence spectra taken from the bottom left area of the protiro and referring to those pixels of the thematic map in **b** where the protective treatment was strongly present (*yellow–red pixels*); and **d** fluorescence spectra taken in the bottom right area of the protiro where the protective treatment is present in a lower degree

cence signature of the protective treatment is present in almost all the spectra (spot 3 and 4 mainly show the fluorescence due to the stone). The 308-nm excitation in the areas affected by the protective treatment yields a peak at about 380 nm.

Figure 9a presents a picture of the right portal of the cathedral (area J in Fig. 1a and Table 1). This area of the facade features several different lithotypes, such as ostia sandstone, bardiglio marble, sporno sandstone, pietraforte sandstone, etc. Figure 9b shows the relative thematic map for biodeteriogens colonisation. The blue areas indicate the presence of the biodeteriogens. The map was obtained with PCA in the spectral range 650 to 710 nm. This range was chosen to select the chlorophyll fluorescence band.

A picture of the balustrade (area L in Fig. 1b and Table 1) on the roof of the baptistery is shown in Fig. 10a. Figure 10b shows the map of the ratio between the PC2 and PC1 scores: yellow-red areas indicate stones colonised by biodeteriogens. The shape of PC2 is actually associated with the chlorophyll fluorescence spectral shape, while the shape of PC1 is clearly related to the fluorescence of the substrate. In this image the laser beam is not normal to the scanned surface due to the large pointing angle.

Figure 11a shows a picture of the lunette (area C in Fig. 1b and Table 1) of the main portal of the baptistery. The lunette hosts several sacred figures with blue decorations: one type of blue decoration is made of azurite; other blue decorations are made of lapis lazuli. Lapis lazuli is more precious than azurite and was used by the artist for decorating only the most important figure, the Madonna. The thematic map obtained with the PCA technique (Fig. 11b) points out some homogeneous blue areas around the Madonna figure that could be due to the presence of lapis lazuli. The thematic map was obtained as a ratio between the PC4 and the PC1 scores. The PCs (Fig. 11c) were calculated in the range 400 to 700 nm.

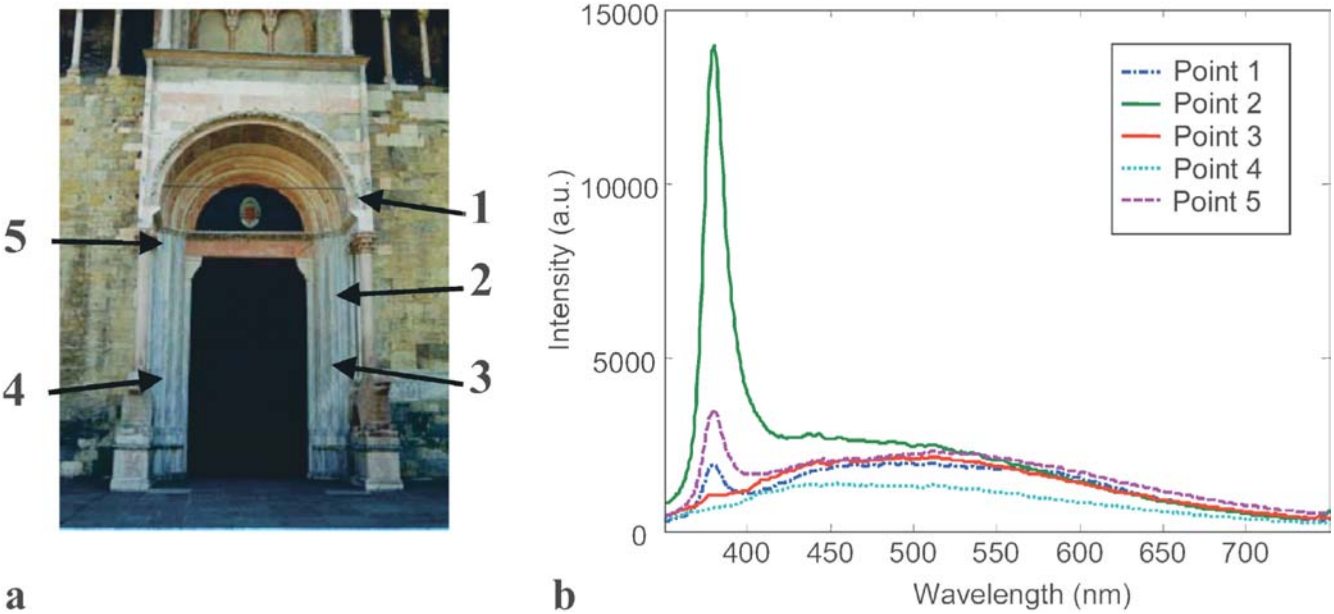

FIGURE 8 Point fluorescence spectra taken in the area around the protiro of the cathedral: **a** a picture of the area investigated with marked *spots* where the measurements were taken; and **b** corresponding fluorescence spectra excited at 308 nm

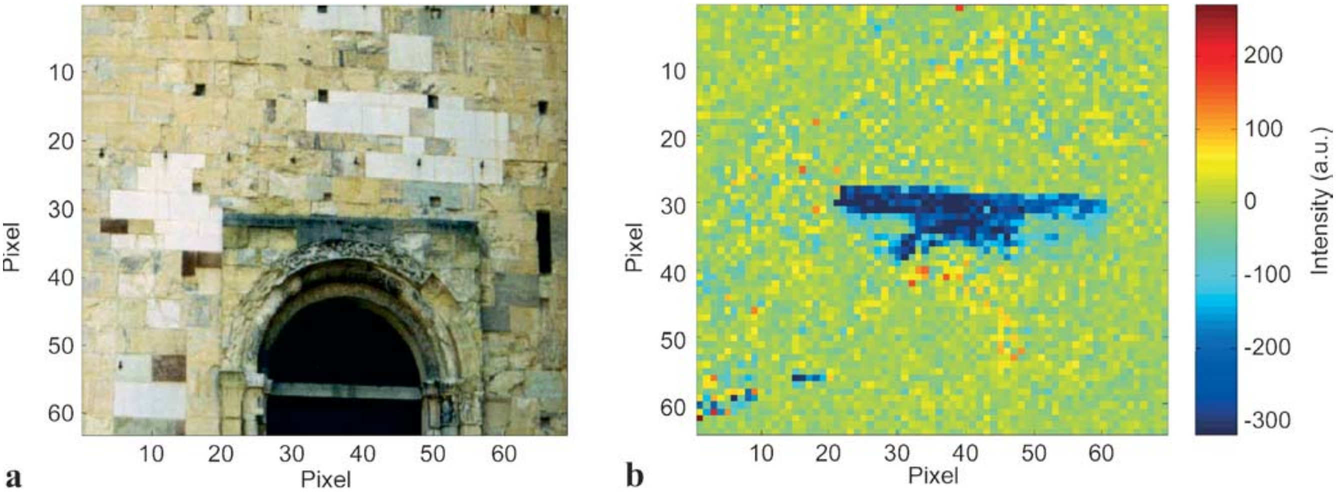

FIGURE 9 Area J of the cathedral: **a** a picture of the area investigated; and **b** the thematic map obtained with PCA in the range 650 to 710 nm; *blue areas* indicate stones affected by the colonisation of biodeteriogens

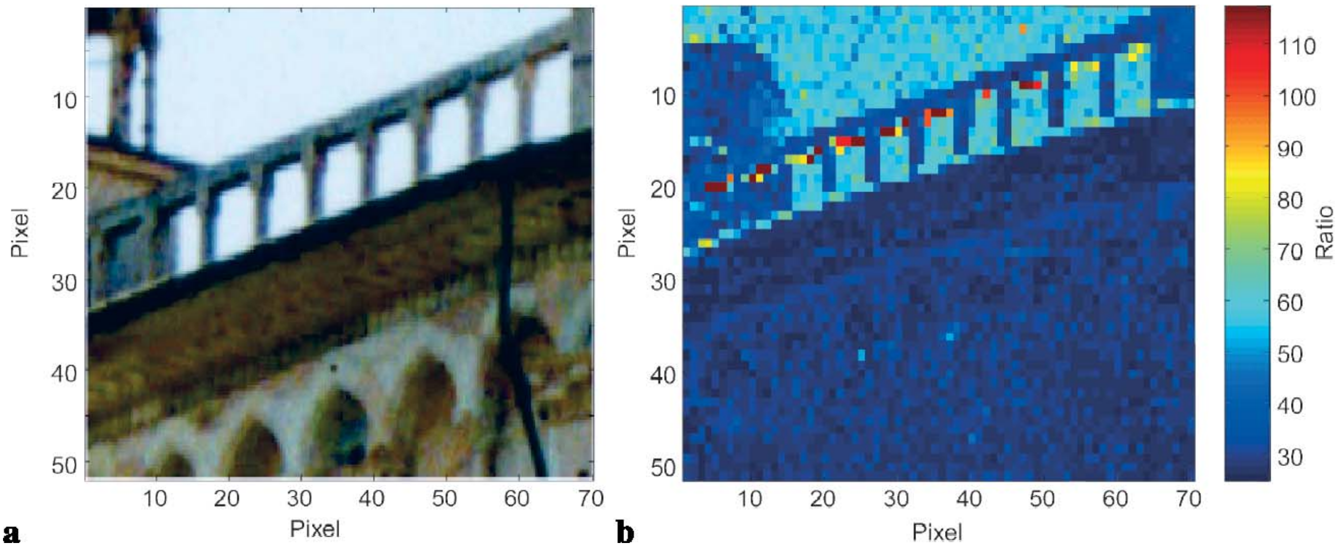

FIGURE 10 Area L of the baptistery balustrade: **a** a picture of the area investigated; and **b** the thematic map obtained by calculating the ratio between the PC2 and PC1 scores; the PCA was performed in the region 400 to 700 nm; *yellow-red areas* in the image indicate stones colonised by biodeteriogens

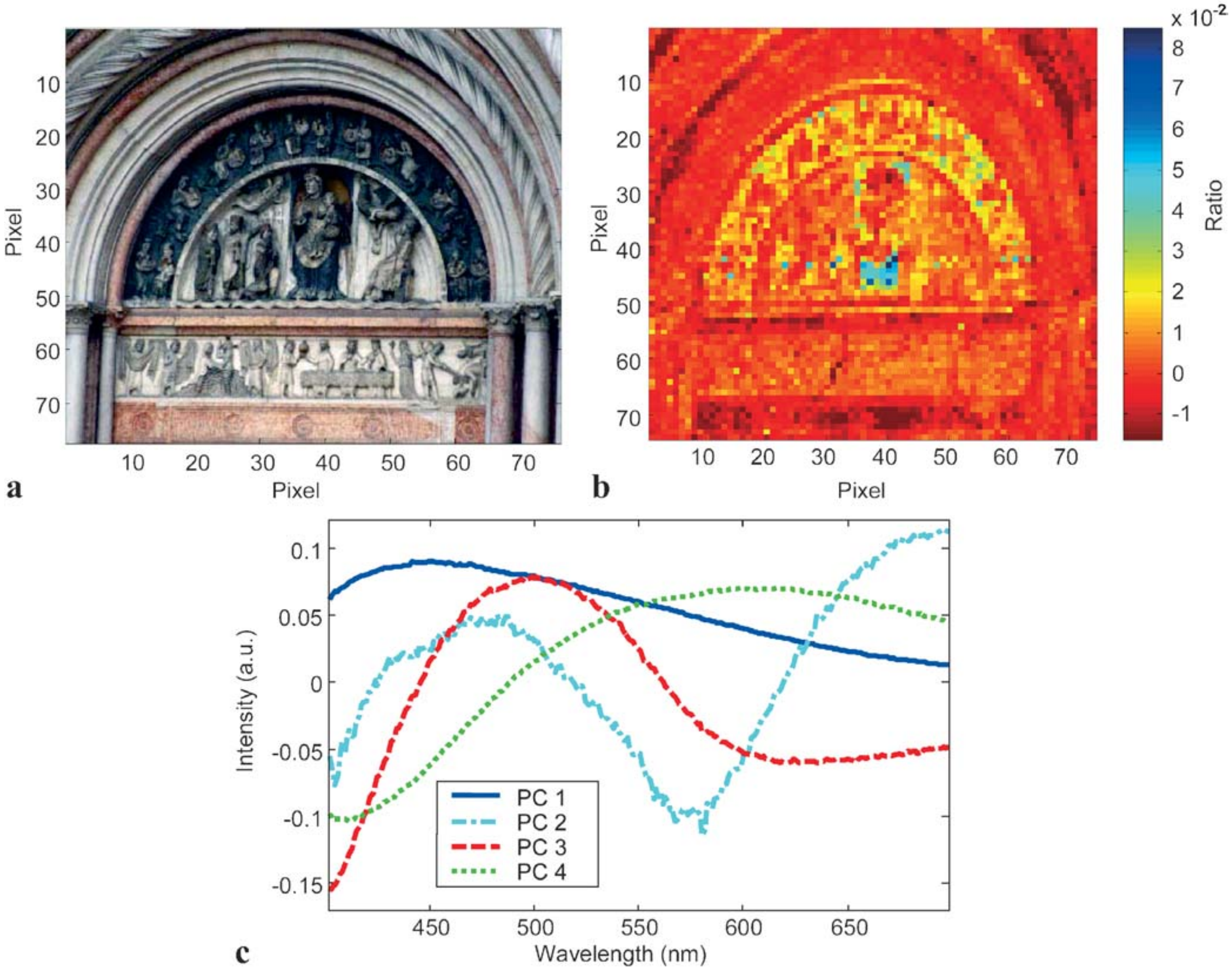

FIGURE 11 Area C of the baptistery: **a** a picture of the area investigated; **b** the thematic map obtained by calculating the ratio between the PC4 and PC1 scores; and **c** shapes of the PC1, PC2, PC3 and PC4; the PCs were calculated in the range 400 to 700 nm

5 Conclusions

Multispectral fluorescence imaging data were obtained from several areas of the cathedral and the baptistery of Parma, Italy, with a mobile lidar system. The experiment has demonstrated the practicability of extensive monitoring of historical buildings with thematic maps. In particular, the thematic maps obtained from the cathedral and the baptistery were first used to outline the presence of areas subject to protective treatment and to biological growth.

Future work will address the geometric rectification of the data, as in satellite imaging, and the investigation of the proper pixel size on the target with respect to the scenario, as in the case of small areas with high resolution, which may be better recorded with non-scanning lidar imaging [20].

ACKNOWLEDGEMENTS This project was supported by the EU-IHP Access to Large-Scale Infrastructure Programme, Contract No. HPRI-CT-1999-00041, the Knut and Alice Wallenberg Foundation and the CNR Special Project Safeguard of the Cultural Heritage Programme. The authors thank the Fabriceria del Duomo di Parma for authorisation to carry out the lidar measurements and for the logistic support supplied in the field.

REFERENCES

1 S. Svanberg: ‘Laser Fluorescence Spectroscopy in Environmental Monitoring’ In *Optoelectronics for Environmental Science*, ed. by S. Martellucci, A.N. Chester (Plenum Press, New York 1990)
2 A.S. Marfunin: *Spectroscopy, Luminescence and Radiation Centers in Minerals* (Springer-Verlag, Berlin 1979)
3 V. Zafiropulus, C. Fotakis: ‘Lasers in the Conservation of Painted Artwork’ In *Laser Cleaning in Conservation: An Introduction*, ed. by M. Cooper (Butterworth Heinemann, Oxford 1998)
4 C.B. Fliermans, E.L. Schmidt: J. Phycology **13**, 364 (1977)
5 R.M. Measures: *Laser Remote Sensing: Fundamentals and Applications* (Wiley, New York 1984)
6 G. Cecchi, L. Pantani, V. Raimondi, D. Tirelli, R. Chiari: Proc. SPIE **2960**, 163 (1996)
7 G. Cecchi, L. Pantani, V. Raimondi, D. Tirelli, R. Chiari, L. Tomaselli, G. Lamenti, M. Bosco, P. Tiano: Proc. SPIE **2960**, 137 (1996)
8 L. Pantani, G. Ballerini, G. Cecchi, H. Edner, D. Lognoli, T. Johansson, V. Raimondi, S. Svanberg, P. Weibring: J. Cultural Heritage **1**, S345 (2000)
9 V. Raimondi, G. Cecchi, L. Pantani, R. Chiari: Appl. Opt. **37**, 1089 (1998)
10 D. Lognoli, G. Lamenti, L. Pantani, D. Tirelli, L. Tomaselli: Proc. SPIE **3868**, 339 (1999)
11 G. Ballerini, S. Bracci, L. Pantani, P. Tiano: Opt. Eng. **40**, 1579 (2001)
12 D. Lognoli, G. Lamenti, L. Pantani, D. Tirelli, P. Tiano, L. Tomaselli: Appl. Opt. LP **41**, 1780 (2002)
13 P. Weibring, T. Johansson, H. Edner, S. Svanberg, B. Sundnér, V. Raimondi, G. Cecchi, L. Pantani: Appl. Opt. LP **40**, 6111 (2001)
14 H. Edner, K. Fredriksson, A. Sunesson, S. Svanberg, L. Unéus, W. Wendt: Appl. Opt. **26**, 4330 (1987)
15 P. Weibring, H. Edner, S. Svanberg: ‘Versatile Mobile Lidar System for Environmental Monitoring’. Appl. Opt. in press
16 K.R. Beebe, B. Kowalski: Anal. Chem. **59**, 1607A (1987)
17 K.V. Mardia, J.T. Kent: *Multivariate Analysis* (Academic Press, London 1979)
18 G. Cecchi, P. Mazzinghi, L. Pantani, R. Valentini, D. Tirelli, P. de Angelis: Rem. Sens. Environ. **47**, 18 (1994)
19 G. Cecchi, L. Pantani, B. Breschi, D. Tirelli, G. Valmori: EARSeL Adv. Rem. Sens. **1**, 72 (1992)
20 H. Edner, J. Johansson, S. Svanberg, E. Wallinder: Appl. Opt. **33**, 2471 (1994)